SMC-TR-03-24

AEROSPACE REPORT NO.
TR-2003(8555)-2

Investigating the High-Rate Discharge Capability of 18650-Type Li-ion Cells

15 June 2003

Prepared by

S. EFTEKHARZADEH and M. L. WASZ
Electronics and Photonics Laboratory
Laboratory Operations

Prepared for

SPACE AND MISSILE SYSTEMS CENTER
AIR FORCE SPACE COMMAND
2430 E. El Segundo Boulevard
Los Angeles Air Force Base, CA 90245

20031001 229

Engineering and Technology Group

THE AEROSPACE CORPORATION
El Segundo, California

APPROVED FOR PUBLIC RELEASE;
DISTRIBUTION UNLIMITED

This report was submitted by The Aerospace Corporation, El Segundo, CA 90245-4691, under Contract No. F04701-00-C-0009 with the Space and Missile Systems Center, 2430 E. El Segundo Blvd., Los Angeles Air Force Base, CA 90245. It was reviewed and approved for The Aerospace Corporation by B. Jaduszliwer, Principal Director, Electronics and Photonics Laboratory. Michael Zambrana was the project officer for the Mission-Oriented Investigation and Experimentation (MOIE) program.

This report has been reviewed by the Public Affairs Office (PAS) and is releasable to the National Technical Information Service (NTIS). At NTIS, it will be available to the general public, including foreign nationals.

This technical report has been reviewed and is approved for publication. Publication of this report does not constitute Air Force approval of the report's findings or conclusions. It is published only for the exchange and stimulation of ideas.

Michael Zambrana

Michael Zambrana
SMC/AXE

REPORT DOCUMENTATION PAGE

Form Approved
OMB No. 0704-0188

Public reporting burden for this collection of information is estimated to average 1 hour per response, including the time for reviewing instructions, searching existing data sources, gathering and maintaining the data needed, and completing and reviewing this collection of information. Send comments regarding this burden estimate or any other aspect of this collection of information, including suggestions for reducing this burden to Department of Defense, Washington Headquarters Services, Directorate for Information Operations and Reports (0704-0188), 1215 Jefferson Davis Highway, Suite 1204, Arlington, VA 22202-4302. Respondents should be aware that notwithstanding any other provision of law, no person shall be subject to any penalty for failing to comply with a collection of information if it does not display a currently valid OMB control number. PLEASE DO NOT RETURN YOUR FORM TO THE ABOVE ADDRESS.

1. REPORT DATE (*DD-MM-YYYY*)
15-06-2003

2. REPORT TYPE

3. DATES COVERED (*From - To*)

4. TITLE AND SUBTITLE

Investigating the High-Rate Discharge Capability of 18650-Type Li-ion Cells

5a. CONTRACT NUMBER
F04701-00-C-0009

5b. GRANT NUMBER

5c. PROGRAM ELEMENT NUMBER

5d. PROJECT NUMBER

5e. TASK NUMBER

5f. WORK UNIT NUMBER

6. AUTHOR(S)

S. Eftekharzadeh and M. L. Wasz

7. PERFORMING ORGANIZATION NAME(S) AND ADDRESS(ES)

The Aerospace Corporation
Laboratory Operations
El Segundo, CA 90245-4691

8. PERFORMING ORGANIZATION REPORT NUMBER

TR-2003(8555)-2

9. SPONSORING / MONITORING AGENCY NAME(S) AND ADDRESS(ES)

Space and Missile Systems Center
Air Force Space Command
2450 E. El Segundo Blvd.
Los Angeles Air Force Base, CA 90245

10. SPONSOR/MONITOR'S ACRONYM(S)
SMC

11. SPONSOR/MONITOR'S REPORT NUMBER(S)
SMC-TR-03-24

12. DISTRIBUTION/AVAILABILITY STATEMENT

Approved for public release; distribution unlimited.

13. SUPPLEMENTARY NOTES

14. ABSTRACT

The high-rate discharge capability of 18650-type lithium-ion cells has been investigated using two commercial cells from Canon battery (A&TB Cells) and Sony, and one space-grade lithium-ion cell. All cells exhibit good voltage stability at various states of charge during pulse application, with Canon (A&TB) cells having the largest drop in voltage. These Canon (A&TB) cells also show the greatest sensitivity to aging with respect to pulse performance, exhibiting irregular voltage signature due to aging. The voltage drop during the pulse load is found to be independent of the pulse rate for all the cells. The voltage drop for the space-grade lithium-ion cell is also independent of the state of charge, exhibiting similar loss at different voltages. The two commercial cells exhibit a higher loss of voltage due to pulse load at lower states of charge. This data indicates that voltage loss at high rates needs to be tested at the lowest state of charge for an intended application. This finding is in contrast with silver-zinc cells, which typically do not have a strong dependence on states of charge.

15. SUBJECT TERMS

High-rate battery, Pulse, Launch vehicle battery, Lithium-ion battery

16. SECURITY CLASSIFICATION OF:			17. LIMITATION OF ABSTRACT	18. NUMBER OF PAGES	19a. NAME OF RESPONSIBLE PERSON
				25	Shirin Eftekharzadeh
a. REPORT	b. ABSTRACT	c. THIS PAGE			19b. TELEPHONE NUMBER (*include area code*)
UNCLASSIFIED	UNCLASSIFIED	UNCLASSIFIED			(310)336-8724

Contents

1. Introduction 1
2. Test Articles 3
3. Test Procedure, Results, and Discussion 5
   - 3.1 Initial Characterization of Commercial Batteries 5
   - 3.2 Cell Characterization 5
     - 3.2.1 Voltage Decay of Fully Charged Cells 6
     - 3.2.2 Capacity Characterization 7
     - 3.2.3 Pulse Characterization 10
4. Final Remarks 23

References 25

Figures

1. Variation of open-circuit voltage of individual cells at room temperature right after charge 7
2. Typical charge-discharge profile of a Sony cell (SB-1 8
3. Typical charge-discharge profile of a Canon (A&TB) cell (CB-1 8
4. Typical charge-discharge profile of the space-grade cell 9
5. Plot presenting the percent of total capacity provided at different discharge rates after cells were fully reconditioned by slower rates discharge steps 9
6. Transient voltage response of Sony SA-2 cell to 2.8-A current 12
7. Transient voltage response of Sony SB-1 cell to 2.8-A current 13
8. Transient voltage response of Canon (A&TB) CB-1 cell to 3-A current 14
9. Transient voltage response of Canon (A&TB) CB-2 cell to 3-A current 15

10. Transient voltage response of the space-grade cell to 2.8-A current 16

11. Plot presenting the instantaneous (0.01 s) and total (1 s) voltage drop after the application of pulse load in Sony SA-2 cell before and after the wake-up characterization cycles..... 17

12. Plot presenting the instantaneous (0.01 s) and total (1 s) voltage drop after the application of pulse load in Sony SB-1 cell before and after the wake-up characterization cycles..... 18

13. Plot presenting the instantaneous (0.01 s) and total (1 s) voltage drop after the application of pulse load in Canon (A&TB) CB-1 cell before and after the wake-up characterization cycles 19

14. Plot presenting the instantaneous (0.01 s) and total (1 s) voltage drop after the application of pulse load in Canon (A&TB) CB-2 cell before and after the wake-up characterization cycles 20

15. Plot presenting the instantaneous (0.01 s) and total (1 s) voltage drop after the application of pulse load in the space-grade cell before and after the wake-up characterization 21

Tables

1. Initial Characterization and Charging Characteristics of Sony NP-F550 Battery 5

2. Initial Characterization and Charging Characteristics of Canon BP-511 Battery 5

3. Variation of Battery Voltage and Impedance With Time After Fully Charged 6

4. Cells Specification After Removal From Each Battery 6

5. Charge and Discharge Capacitates Obtained at Different Rates 10

6. Details of Pulse Characterization Procedure 11

Acknowledgment

The work of Mr. Michael Quinzio in setting up the electrical equipment for fast data acquisition, his assistance in removing the cells, and his instruction in operating the test equipment has been very valuable and is greatly appreciated.

1. Introduction

An investigation has been conducted to examine the high-rate discharge capability of 18650-type lithium-ion cells for use in launch vehicle applications. Two commercially available cells from Canon and Sony batteries and one space-qualified lithium-ion cell have been selected for this work. The ability to maintain voltage for pulse rates of up to 3C has been evaluated at different states of charge. The effect of fully charged open-circuit voltage stand at room temperature prior to pulse application has also been investigated.

2. Test Articles

The commercial lithium-ion cells were obtained from Sony and Canon batteries used in digital still and video cameras. These batteries provide power to the built-in flash while maintaining normal functioning of the camera. Batteries were purchased in August of 2002 with the following characteristics:

(1) Canon lithium-ion battery part # BP-511; 7.4 V and manufacturer-rated capacity of 1.1 Ah.

This battery is used in Canon's Powershot G1 digital camera. The battery was expected to have two 3.7-V, 1.1-Ah cells connected in series. The manufacturer's recommended operating and charging temperature was 0°C to 40°C with better operating performance at 10°C to 30°C. According to the manufacturer, charging time was longer at warmer temperatures, and operating time shorter at low temperatures. Temperatures greater than 60°C were not recommended. The charger's rated output was 8.4 V and 2.5 A.

(2) Sony lithium-ion battery part # NP-F550, 7.2 V and manufacturer-rated capacity of 1.5 Ah.

This battery is used in Sony's Cybershot Pro and Mavica digital cameras. The battery was expected to have two 3.6-V, 1.5-Ah cells connected in series. The manufacturer's recommended operating and charging temperature was 0°C to 40°C, but the highest capacity was expected at charging temperature of 10°C–30°C. Battery performance is expected to degrade at low temperatures. Temperatures greater than 60°C were not recommended. The charger's output was 8.4 V and 0.6 A.

(3) Lithium-ion cell designed for space applications, rated at 1.20 Ah.

3. Test Procedure, Results, and Discussion

3.1 Initial Characterization of Commercial Batteries

The voltage and impedance of each battery were measured upon delivery (Table 1 and 2). Each battery was then charged within one week of delivery using the manufacturer-recommended charger. Charging of the Sony battery took place in two stages with the first one described by Sony as the normal charge, and the second stage after one additional hour designated as full charge. Charging for the Canon battery took place in 3 stages of 50%, 75%, and 100% charged. The time, voltage, and impedance of each battery was monitored during each stage and are presented in Tables 1 and 2.

Both batteries were fully charged to 8.4V (±0.05). The average total charge time for the Canon battery was 0.88 hr compared to 2.71 hr for the Sony battery, a factor of 3 shorter for the Canon battery.

Table 1. Initial Characterization and Charging Characteristics of Sony NP-F550 Battery

Sony NP-F550	Initial Voltage (V)	Initial Impedance (Ω)	Time to Reach First Stage of Charge	Voltage at First State of Charge (V)	Impedance at First Stage of Charge (Ω)	Extra Time to Fully Charge Per Manufacturer	Voltage at Full Charge (V)	Impedance at Full Charge (Ω)
Sony A	7.59	0.240	1 h & 45 min (1.75 h)	8.253	0.226	1 h	8.395	0.224
Sony B	7.58	0.270	1 h & 40 min (1.67 h)	8.298	0.225	1 h	8.389	0.223

Table 2. Initial Characterization and Charging Characteristics of Canon BP-511 Battery

Canon BP-511	Initial voltage (V)	Initial impedance (Ω)	Time to reach 50% charged (min)	Voltage when 50% charged	Time to reach 75% SOC (min)	Voltage when75% SOC	Time to reach 100 % SOC (min)	Voltage when 100% SOC	Impedance at 100% SOC
Canon A	7.62	0.217	10	7.99	11	8.243	32	8.447	0.20
Canon B	7.62	0.216	12	8.03	8	8.226	32	8.442	0.188

3.2 Cell Characterization

Individual commercial cells were removed from each battery within one week of charge. The voltage of the battery during this time showed a small change with time, while the impedance remained relatively constant as indicated in Table 3. Table 4 presents individual cell's date codes along with their voltage and impedance after removal from the batteries. Cells removed from the Canon battery appear to be manufactured by A&TB, as indicated by their labels. The voltage of each charged cell was approximately 4.2 V (±0.05). The impedances of Canon (A&TB) cells were on average higher, 0.084 Ω compared to 0.061 Ω for Sony cells.

Table 3. Variation of Battery Voltage and Impedance With Time After Fully Charged

Sony A					
	$t_0 = 0$	t_1 = 16 h & 45 min	t_2 = 40 h & 50 min	t_3 = 113 h & 50 min	t_4 = 139 h
	V = 8.395 V	V = 8.377 V	V = 8.3721 V	V = 8.3613 V	V = 8.3578 V
	R = 0.2243 Ω	V = 0.223 Ω	R = 0.222 Ω	R = 0.223 Ω	R = 0.221 Ω
Sony B					
	$t_0 = 0$	t_1 = 70 h & 25 min	t_2 = 95 h & 40 min		
	V = 8.3885 V	V = 8.3587 V	V = 8.355 V		
	R = 0.223 Ω	R = 0.225 Ω	R = 0.225 Ω		
Canon A					
	$t_0 = 0$	t_1 = 71 h & 45 min	t_2 = 97 h & 15 min		
	V = 8.4467 V	V = 8.3931 V	V = 8.3859 V		
	R = 0.2 Ω	R = 0.1940 Ω	R = 0.192 Ω		
Canon B					
	$t_0 = 0$	t_1 = 71 h & 10 min	t_2 = 97 h & 10 min		
	V = 8.4420 V	V = 8.3914 V	V = 8.3844 V		
	R = 0.188 Ω	R = 0.204 Ω	R = 0.186 Ω		

Table 4. Cells Specification After Removal From Each Battery

Sony Fukushima Us18650gr	Cell ID	Voltage (V)	Impedance (Ω)	Weight (g)
SA-1	STG 5KE08D	4.173	0.063	45.0
SA-2	STG 5KE08D	4.177	0.059	45.5
SB-1	STG 5KE08D	4.177	0.061	45.1
SB-2	STG 5KE08D	4.177	0.061	45.2
Canon BP-511 A&TB				
CA-1	857105714 LGR18500P	4.193	0.086	32.4
CA-2	857105750 LGR18500P	4.181	0.091	32.4
CB-1	857122921 LGR18500P	4.191	0.088	32.4
CB-2	857122902 LGR18500P	4.184	0.071	32.4

3.2.1 Voltage Decay of Fully Charged Cells

The voltage of fully charged cells was monitored as a function of time under ambient condition. The voltage of the space-grade cell was also monitored after a 20-mA charge to 4.16 V (prior to this, the

space-grade cell sat open circuit in a discharged state for 57 days upon receipt, plus an additional 30 days after a 20-mA charge to 4.05 V). Figure 1 presents the variation of voltage with time for each charged cell. In general, Canon (A&TB) cells showed a greater rate of self-discharge at 4.2 V compared to Sony cells. The space-grade and Sony cell showed a relatively similar variation in voltage with time, with the space-grade cell having a slightly slower rate of decay.

3.2.2 Capacity Characterization

The capacity of each cell was examined at different charge and discharge rates. Each cell was charged or discharged at the desired rate, followed by subsequent lower rate charge or discharge steps to recondition the cell. The sequence of steps was 2.72C (or 2.50C for space-grade cell), 1.82C, 0.91C, 0.46C, and 0.18C. Figures 2–4 present typical charge-discharge profiles of all the cells from 2.7 V to 4.2 V. Each curve on the plot presents the 3rd charge or discharge curve after the cell is fully conditioned by lower rate charge or discharge steps. Both Canon (A&TB) and Sony cells exhibit a relatively flat discharge voltage curve with a sharp knee bend, followed by a quick voltage drop before the discharge cut off voltage. The flat discharge curve is a typical behavior of graphite anodes, and thus the anode in these cells is believed to be graphite. The discharge capacity-voltage profile of the space-grade cell is different, showing a continuous and gradual drop in voltage from 4.2 V to 2.7 V. This behavior is typical to coke anodes, and thus the anode for the space-grade cell is believed to be an amorphous carbon.

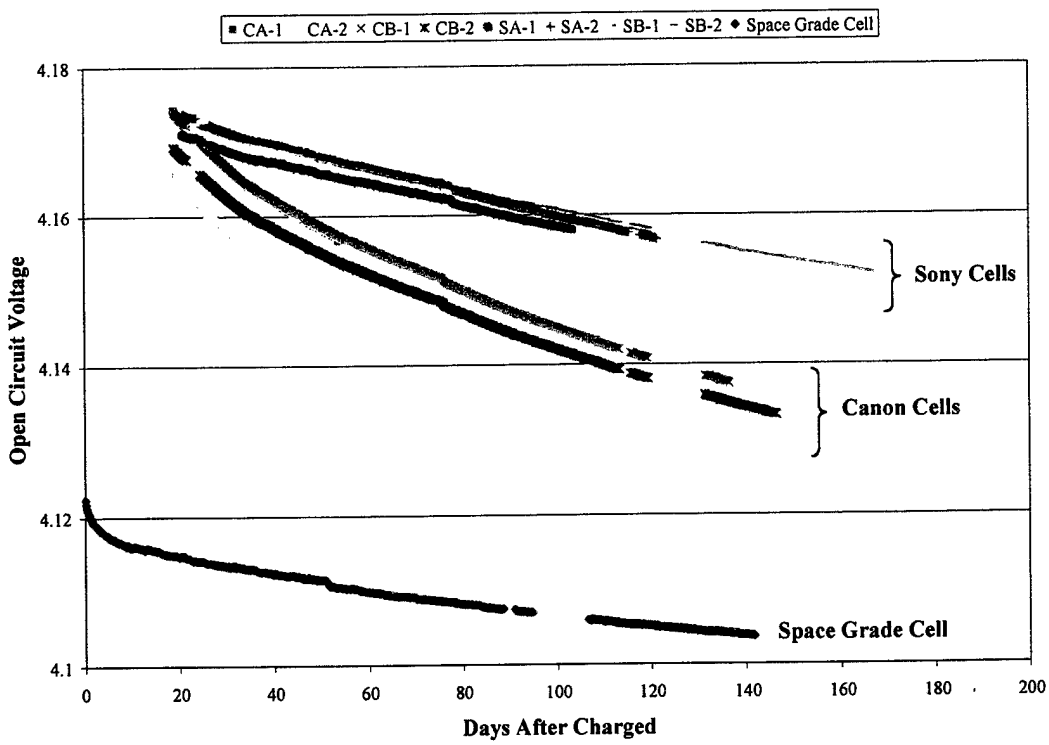

Figure 1. Variation of open-circuit voltage of individual cells at room temperature right after charge.

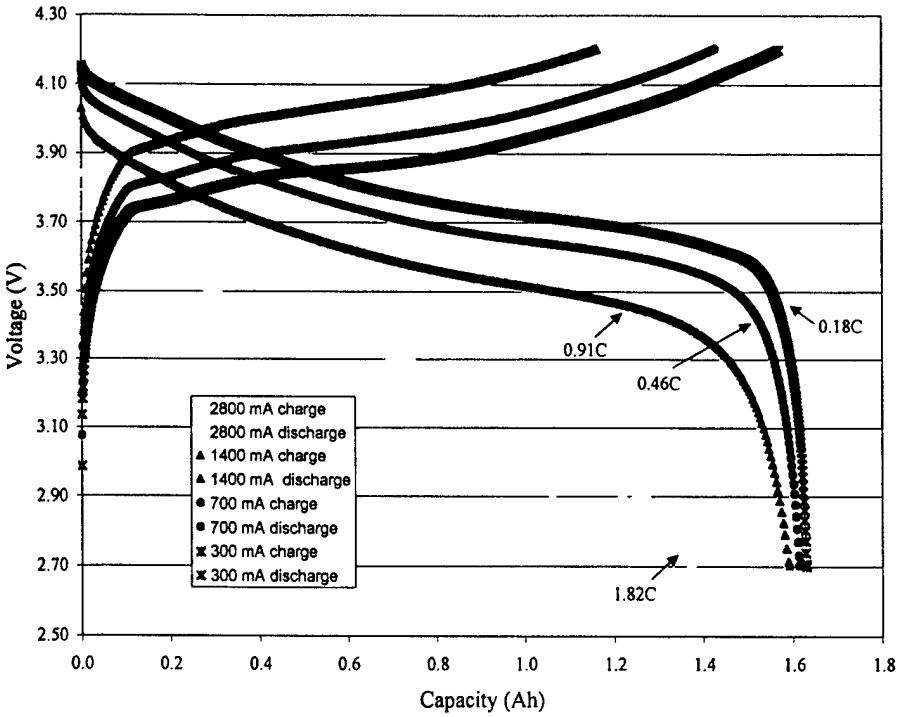

Figure 2. Typical charge-discharge profile of a Sony cell (SB-1); "C" is based on the rated capacity of 1.6 Ah.

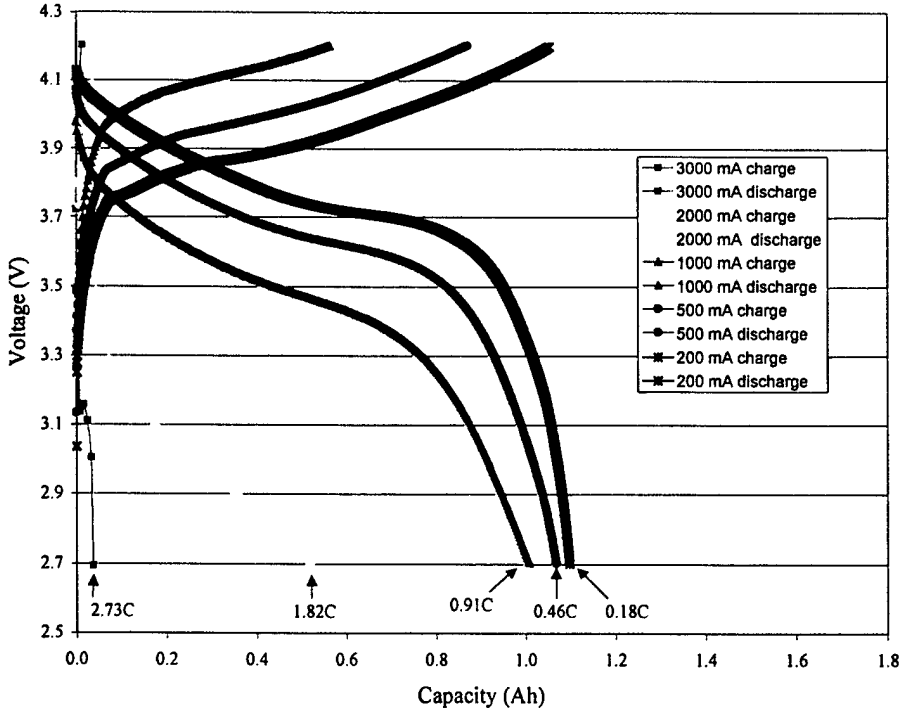

Figure 3. Typical charge-discharge profile of a Canon (A&TB) cell (CB-1); "C" is based on the rated capacity of 1.1 Ah.

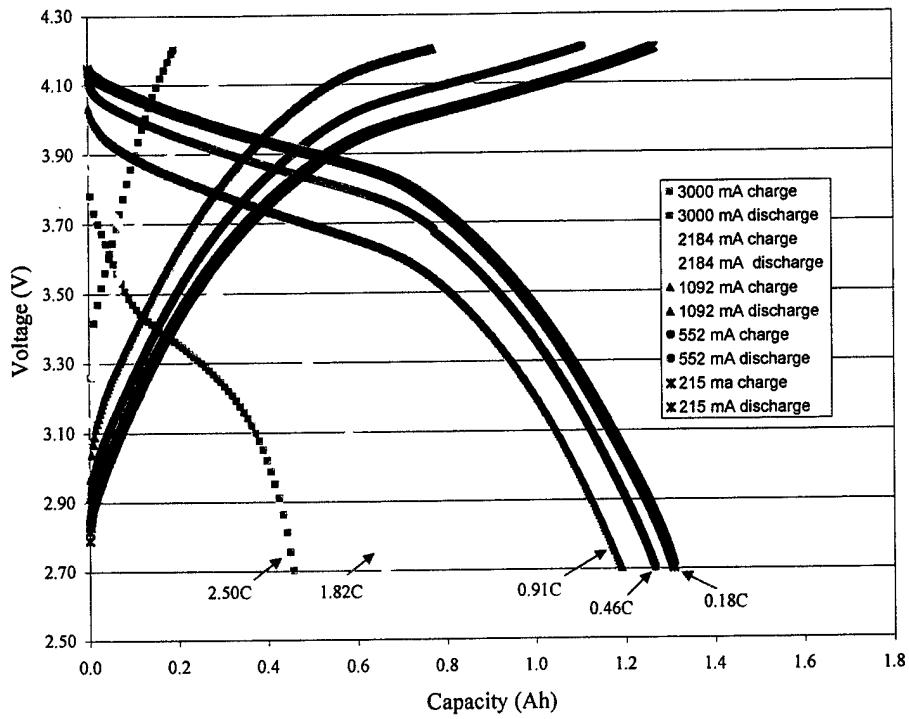

Figure 4. Typical charge-discharge profile of the space-grade cell. "C" is based on the rated capacity of 1.2 Ah.

Figure 5 presents the percent of discharge capacities delivered at different rates relative to the lowest rate discharge capacity tested (or total capacity). Table 5 also summarizes these results for both charge and discharge after cells are reconditioned by slower rate steps. The Sony cell showed the

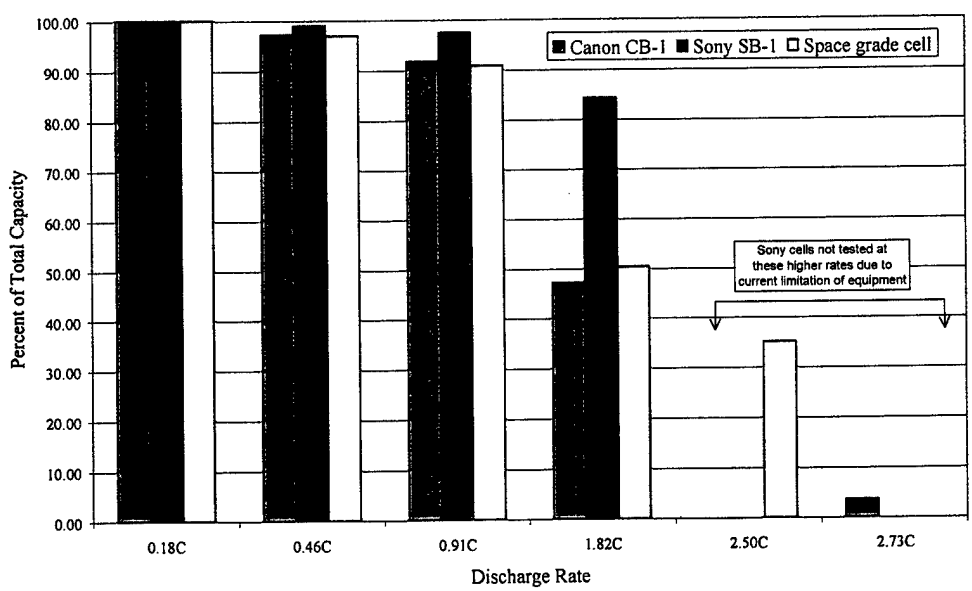

Figure 5. Plot presenting the percent of total capacity provided at different discharge rates after cells were fully reconditioned by slower rates discharge steps.

Table 5. Charge and Discharge Capacitates Obtained at Different Rates. Cells are reconditioned prior to each charge or discharge by slower rate charge or discharge steps.

Discharge Rate	Charge Capacity CB-1 (Ah)	% of Total Charge Capacity CB-1	Discharge Capacity CB-1 (Ah)	% of Total Discharge Capacity CB-1	Charge Capacity SB-1 (Ah)	% of Total Charge Capacity SB-1	Discharge Capacity SB-1 (Ah)	% of Total Discharge Capacity SB-1	Charge Capacity Space-Grade Cell (Ah)	% of Total Charge Capacity Space-Grade Cell (Ah)	Discharge Capacity Space-Grade Cell (Ah)	% of Total Discharge Capacity Space-Grade Cell (Ah)
0.18C	1.05	100.00	1.10	100.00	1.57	100.00	1.63	100.00	1.27	100.00	1.31	100.00
0.46C	0.87	82.54	1.07	97.27	1.43	90.89	1.61	99.02	1.11	87.40	1.27	96.95
0.91C	0.57	53.61	1.01	91.70	1.16	74.01	1.59	97.55	0.78	61.42	1.19	90.84
1.82C	0.05	4.84	0.52	47.13	0.28	17.90	1.37	84.23	0.35	27.56	0.66	50.38
2.50C									0.19	14.96	0.46	35.11
2.73C	0.02	1.42	0.04	3.56								

best performance with respect to discharge capacity at higher rates, delivering almost 84% capacity at 1.82C compared to 47% for Canon (A&TB) and 50% for the space-grade cell. The Canon (A&TB) cell showed the poorest charging performance at higher rates. It is believed that the manufacturer's faster charging time for Canon (A&TB) cell is unrelated to its charging capability and is mainly driven by consumer demand and the desire to charge batteries fast.

3.2.3 Pulse Characterization

The pulse performance of each cell was investigated by monitoring the transient voltage response to the pulse load at different states of charge. This characterization was performed initially after the fully charged stand at room temperature without reconditioning. This was done to examine the effect of aging on pulse performance. Cells were tested individually at different times, from 119 days to 144 days, due to equipment limitation. Each cell was placed in a 20°C isothermal bath for a minimum of 2 h prior to testing. Pulse characterization testing for all the cells involved:

(1) An initial charge to 4.2 V followed by 1-h open-circuit stand. Charge rates were 200 mA for Canon (A&TB) and 300 mA for Sony and the space-grade cells.

(2) Application of pulse current, 3.0 A for Canon (A&TB) and 2.8 A for Sony and the space-grade cells. Pulse duration was 1 s.

(3) Discharge to the desired voltage followed by 1-h open-circuit stand at each state of charge. Discharge rates were 200 mA for Canon (A&TB) and 300 mA for Sony and the space-grade cells. The ends of discharge voltage limits were 4.0, 3.8, 3.6, 3.4, 3.2, 3.0, and 2.8 V.

(4) Application of pulse current, 3.0 A for Canon (A&TB) and 2.8 A for Sony and the space-grade cells. Pulse duration was 1 s.

Once the initial pulse characterization was completed, cells were reconditioned by applying several wake-up cycles. The wake-up cycles served both as a mean of re-reconditioning the cell and also examining the cell's charge and discharge capability at different rates without being reconditioned. These cycles included 3 charge-discharge steps at 1000, 500, and 200 mA for Canon (A&TB) and 3 charge-discharge steps at 1400, 700, and 300 mA for Sony and the space-grade cells. Pulse charac-

terization was repeated after the completion of the wake-up cycles at the initial tested current. This characterization was also repeated at half the initial rate to examine any dependence of voltage drop to current. A summary of the pulse characterization steps is presented in Table 6.

Figures 6–10 present the transient voltage response of the cells before and after wake-up cycles during the 1-s pulse application. Figures 11–15 plot the instantaneous voltage drop right after pulse application and the total voltage drop after the 1-s period at different states of charge. The first observation made from these results is that, for similar pulse rates, Canon (A&TB) cells show an overall greater drop in voltage compared to the other cells. This is expected since the impedance of Canon (A&TB) cells is on average higher, 0.084 Ω compared to 0.061 Ω for Sony cells and 0.066 Ω for the space-grade cell. The pulse results after wake-up cycles also do not show a direct correlation of the voltage drop to pulse current up to the 3 A maximum current investigated in this work (Figures 11–15). This indicates that the drop of voltage due to a higher rate current is not simply by an ohmic [I(current)*R(resistance)] effect caused by factors such as thin insulative film on the electrode surfaces; but other factors are also involved. Cells also showed differences with respect to the effect of state of charge on voltage drop. For Canon (A&TB) and Sony cells, the voltage drop due to pulse load shows strong dependence on the state of charge in the region 3.5 V < V < 3.9 V, while the voltage drop for the space-grade cell is independent of the state of charge and remains constant at all voltages (Figures 11–15). This behavior could be attributed to the sharp knee bend in the discharge capacity profile of the Canon (A&TB) and Sony cell, assuming a graphite anode, which occurs in a similar voltage regime (3.5 V < V < 3.9 V), while the discharge capacity profile of the space-grade cell shows a more gradual and somewhat constant change with voltage (Figures 2–4).

Another observation is the difference in aging of Canon (A&TB) cells versus Sony and the space-grade cells. For Sony and the space-grade cells, the transient voltage responses before and after the wake-up cycles at different states of charge show a similar and predictable trend, with an initial quick drop in the voltage followed by a gradual and slow decay through the 1-s pulse period (Figures 6, 7, and 10). Both Sony and the space-grade cells show a slightly smaller voltage drop after the wake-up cycles indicating some signs of aging during the fully charged stand, but this effect is minimal (Figures 11, 12, and 15). Aging appears to have a more pronounced effect on Canon (A&TB) cells. The transient voltage response of Canon (A&TB) cells to pulse load before the wake-up cycles does not follow the same trend at different states of charge and is somewhat unpredictable (Figures 8, 9). Reconditioning appears to stabilize the cell since the voltage response to pulse load at different states of charge becomes more stable and fairly predictable after the wake-up cycles. The voltage drop of Canon (A&TB) cells due to pulse load after the wake-up cycles is also significantly lower than that before re-conditioning (Figures 13, 14). These indicate the sensitivity of Canon (A&TB) cells to aging.

Table 6. Details of Pulse Characterization Procedure. C rates are based on the rated capacities of 1.1 Ah for Canon (A&TB), 1.6 Ah for Sony, and 1.2 Ah for the space-grade cell.

Cell	Charge & Discharge Rates (mA)	Pulse Current Before Wake-up Cycles	Wake-up Cycles	Pulse Current After Wake-up Cycles
Sony	300	2.8 A (1.75C)	3 cycles at 1400, 700, and 300 mA	2.8 A (1.75C) A, 1.4 A (0.5C)
Canon (A&TB)	200	3.0 A (2.73C)	3 cycles at 1000, 500, and 200 mA	3.0 A (2.73C), 2.0 A (1.82C), 1.0A (0.91C)
Space-grade cell	300	2.8 A (2.33C)	3 cycles at 1400, 700, and 300 mA	2.8 A (2.33C), 1.4 A (1.17C)

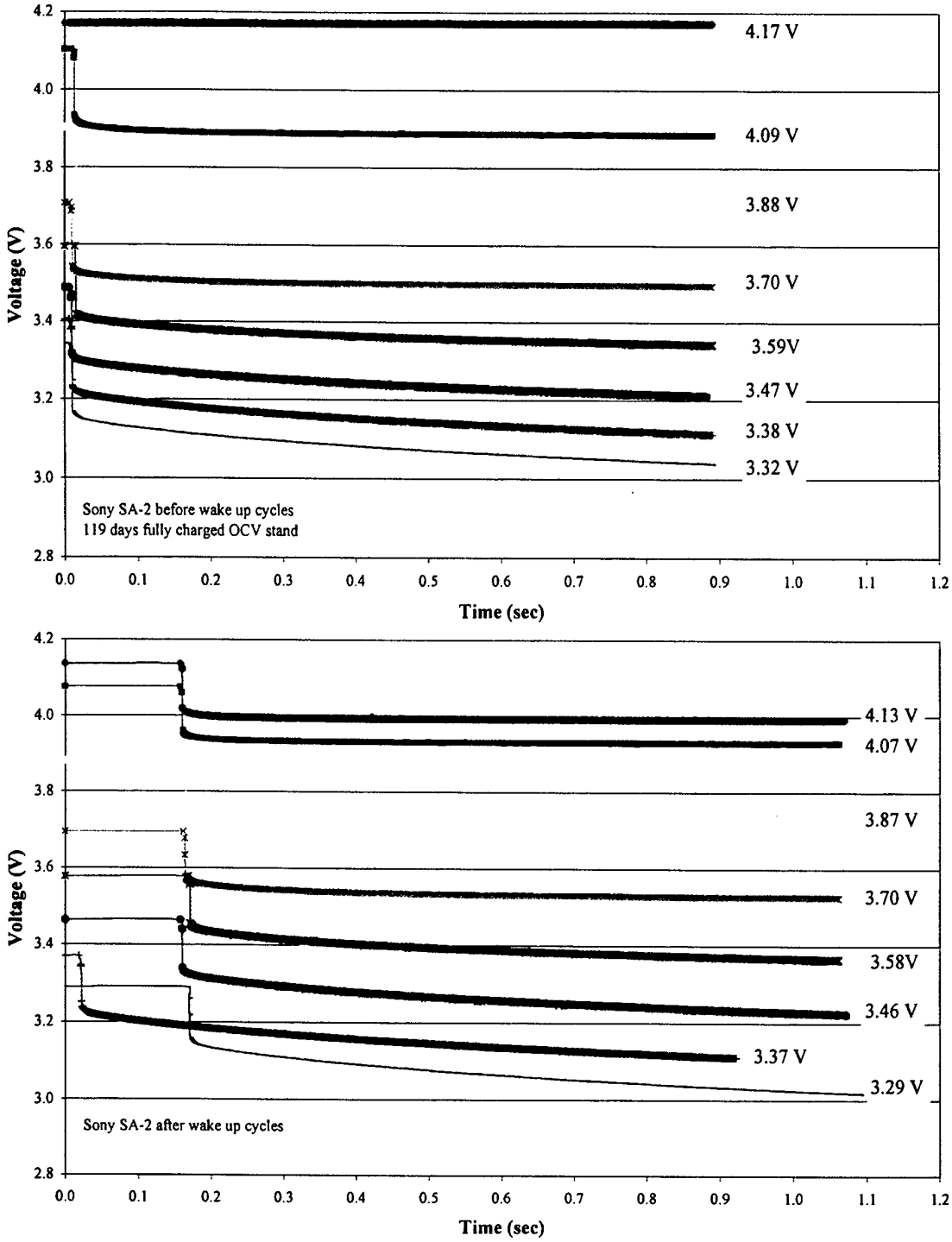

Figure 6. Transient voltage response of Sony SA-2 cell to 2.8-A current; (top) before wake up characterization cycle; (bottom) after wake up characterization cycle

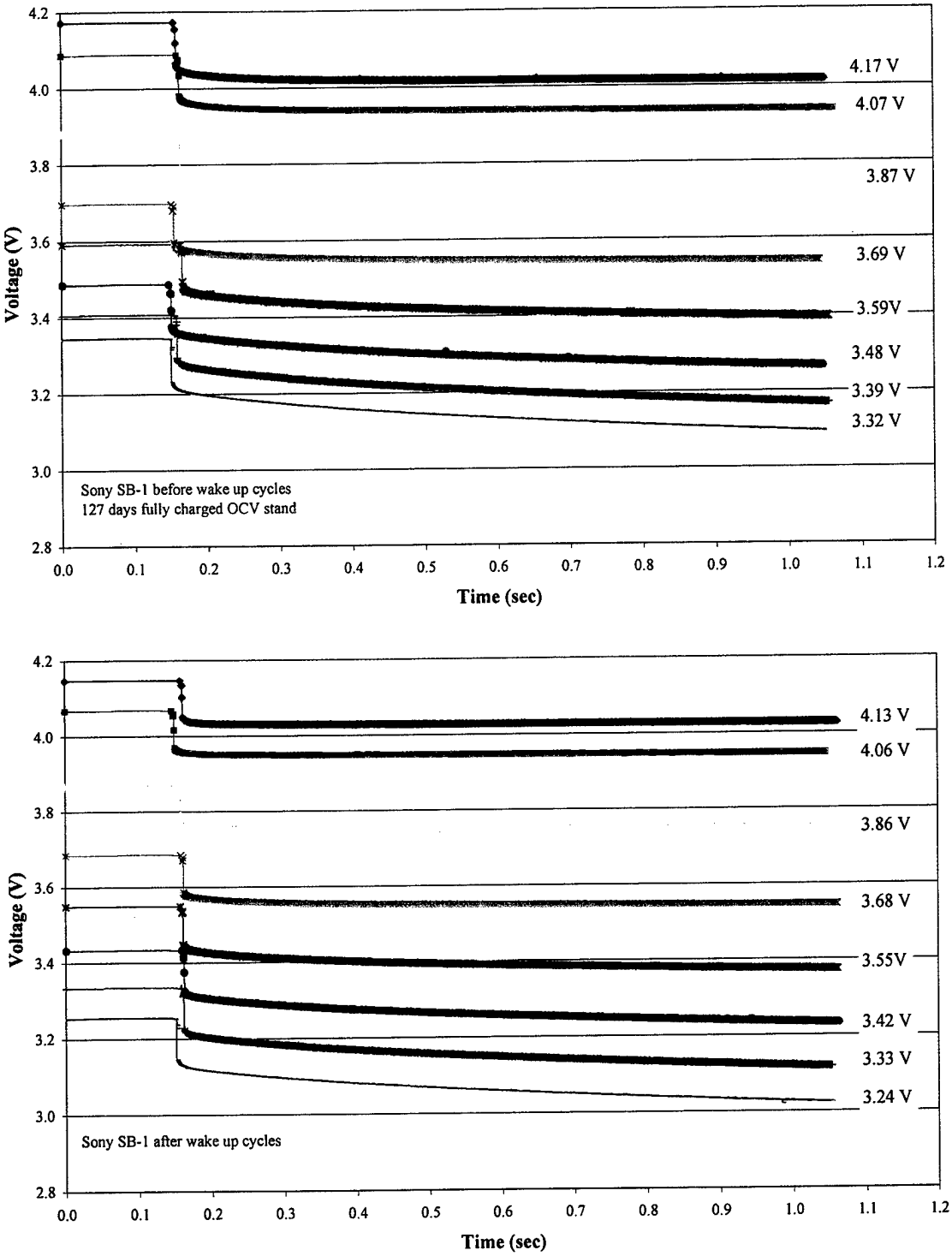

Figure 7. Transient voltage response of Sony SB-1 cell to 2.8-A current; (top) before wake-up characterization cycle; (bottom) after wake-up characterization cycle

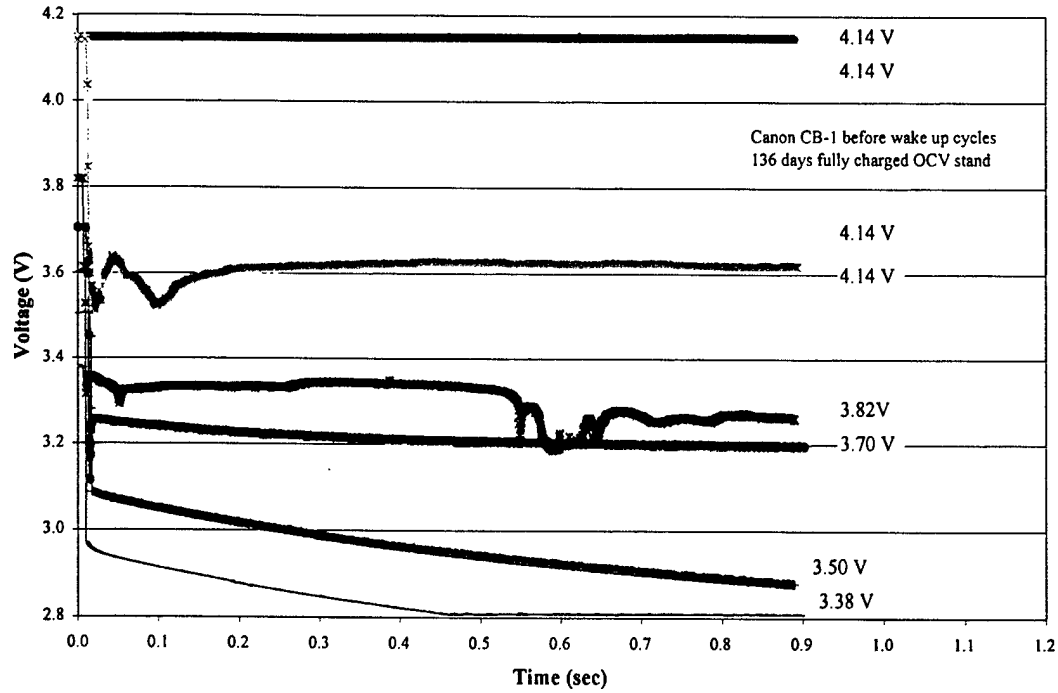

Note: For the aged cell before the wake-up cycles, the first four steps involving 200-mA charge to 4.2 V and 200-mA discharge to 4.0 V, 3.8 V, and 3.6 V, followed by a 3600-s OCV stand lead to similar cell voltages of 4.14 V before the application of pulse current. The cell voltage during each charge or discharge step reached the EOCV or EODV limits very quickly, and the voltage stabilized to 4.14 V during the OCV stand. This may be due to the presence of insulating films on the electrode surfaces formed during the storage period.

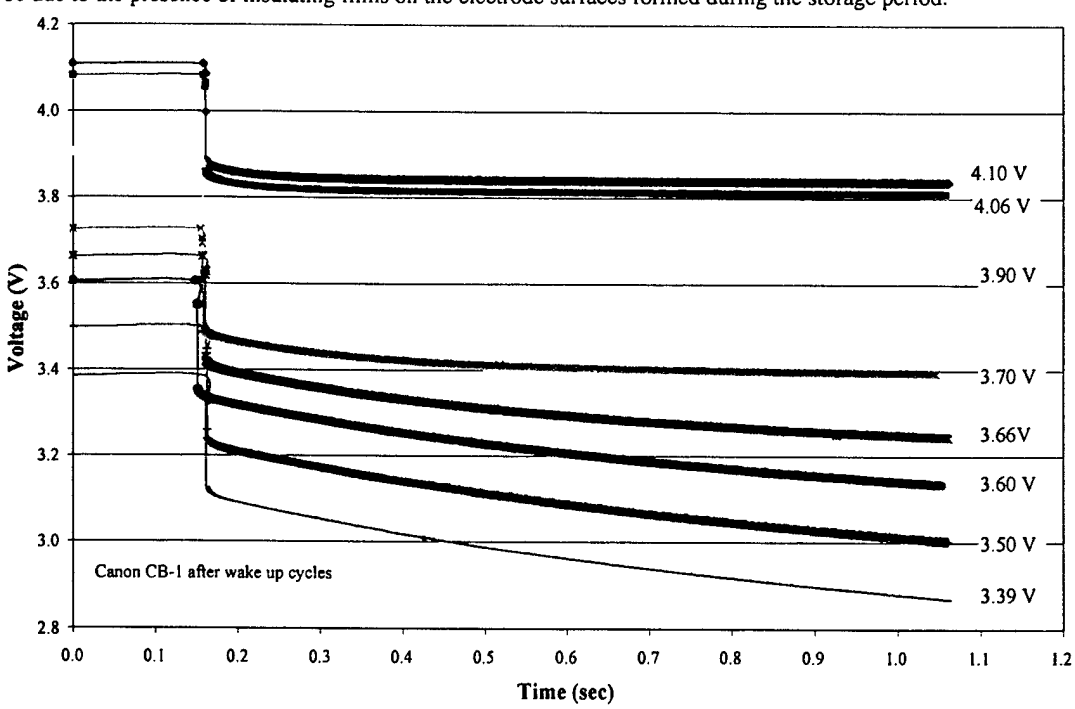

Figure 8. Transient voltage response of Canon (A&TB) CB-1 cell to 3-A current; (top) before wake-up characterization cycle; (bottom) after wake-up characterization cycle

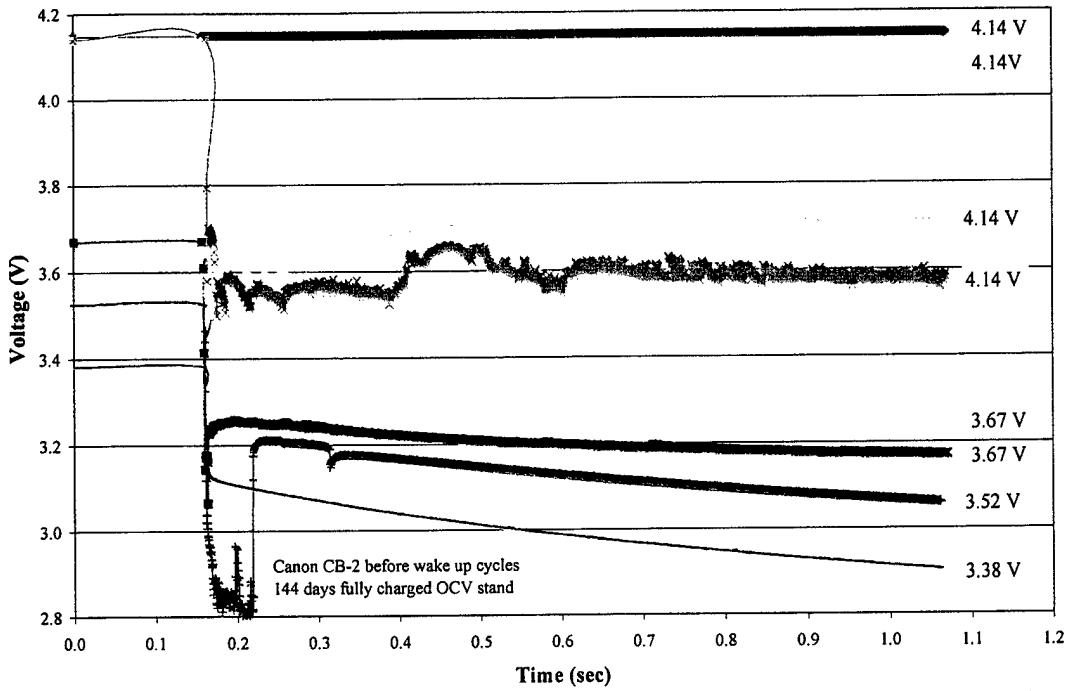

Note: For the aged cell before the wake-up cycles, the first four steps involving 200-mA charge to 4.2 V and 200-mA discharge to 4.0 V, 3.8 V, and 3.6 V, followed by 3600-s OCV stand lead to similar cell voltages of 4.14 V before the application of pulse current. The cell voltage during each charge or discharge step reached the EOCV or EODV limits very quickly and the voltage stabilized to 4.14 V during the OCV stand. This may be due to the presence of insulating films on the electrode surfaces formed during the storage period.

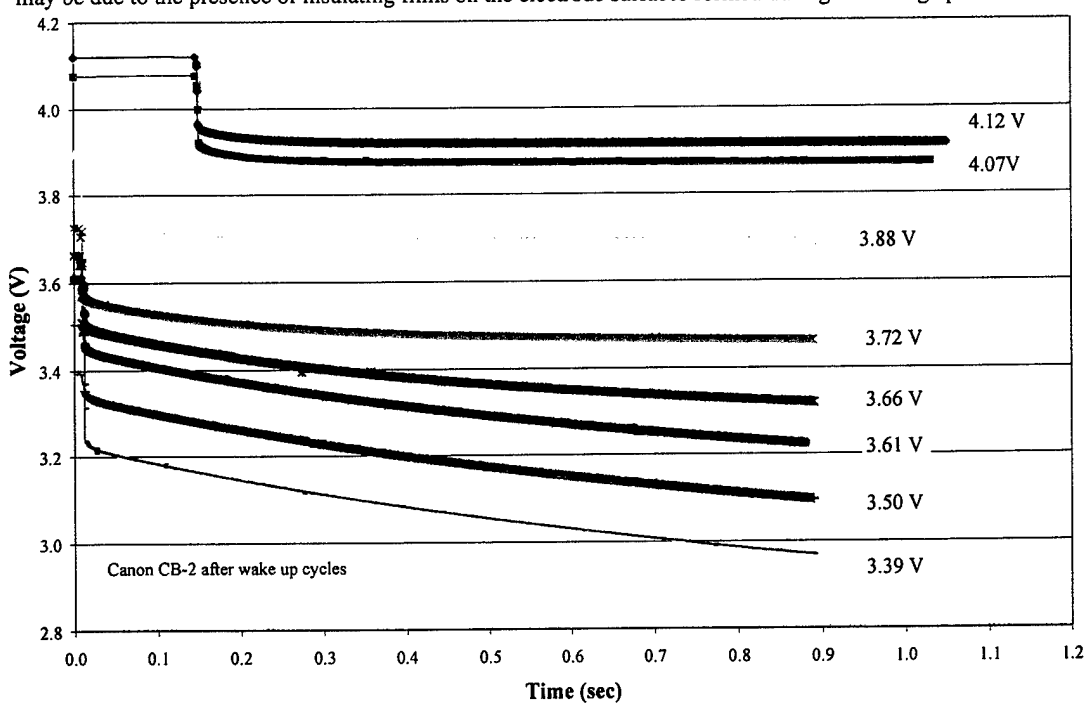

Figure 9. Transient voltage response of Canon (A&TB) CB-2 cell to 3-A current; (top) before wake-up characterization cycle; (bottom) after wake-up characterization cycle.

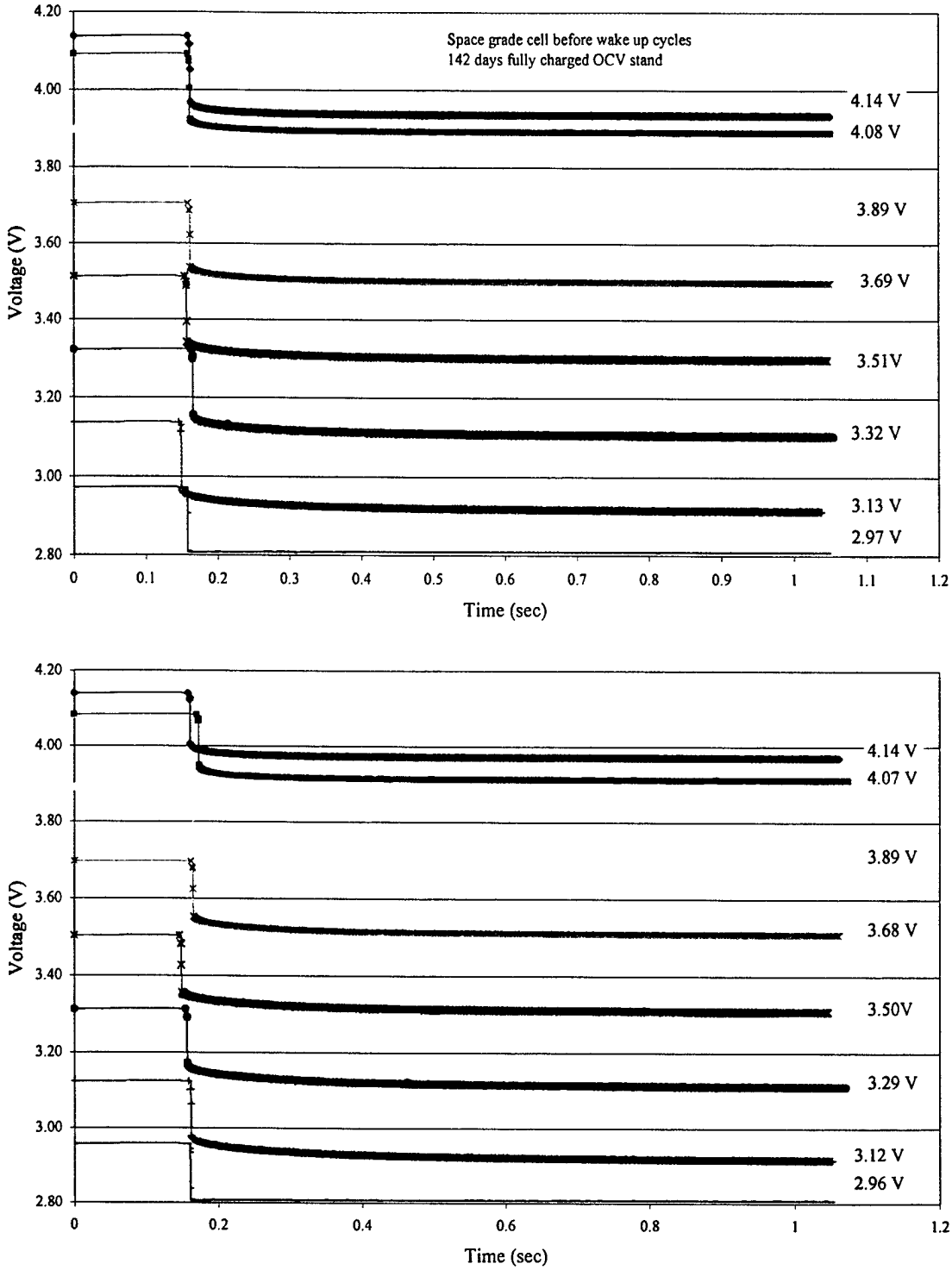

Figure 10. Transient voltage response of the space-grade cell to 2.8-A current; (top) before wake-up characterization cycle; (bottom) after wake-up characterization cycle.

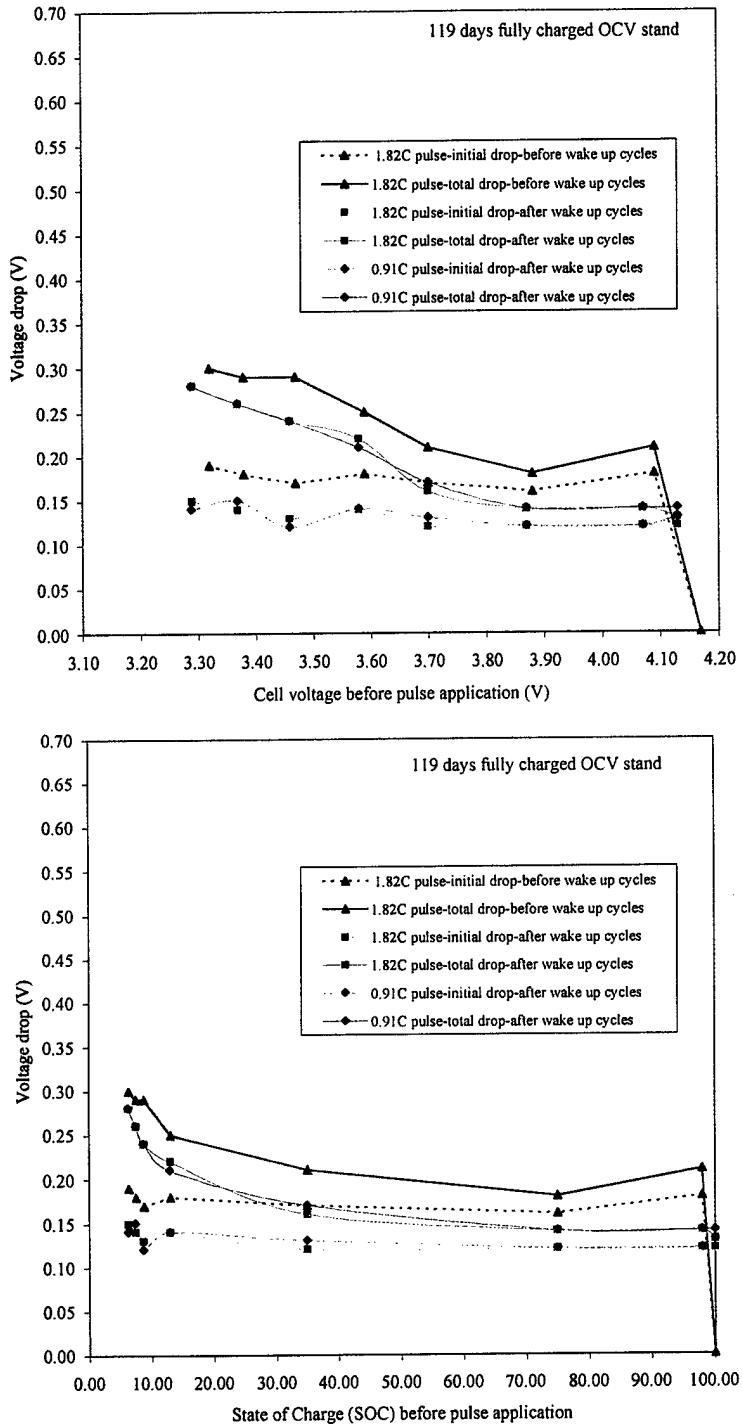

Figure 11. Plot presenting the instantaneous (0.01 s) and total (1 s) voltage drop after the application of pulse load in Sony SA-2 cell before and after the wake-up characterization cycles; (top) plot vs. voltage; (bottom) plot vs. SOC (±5%).

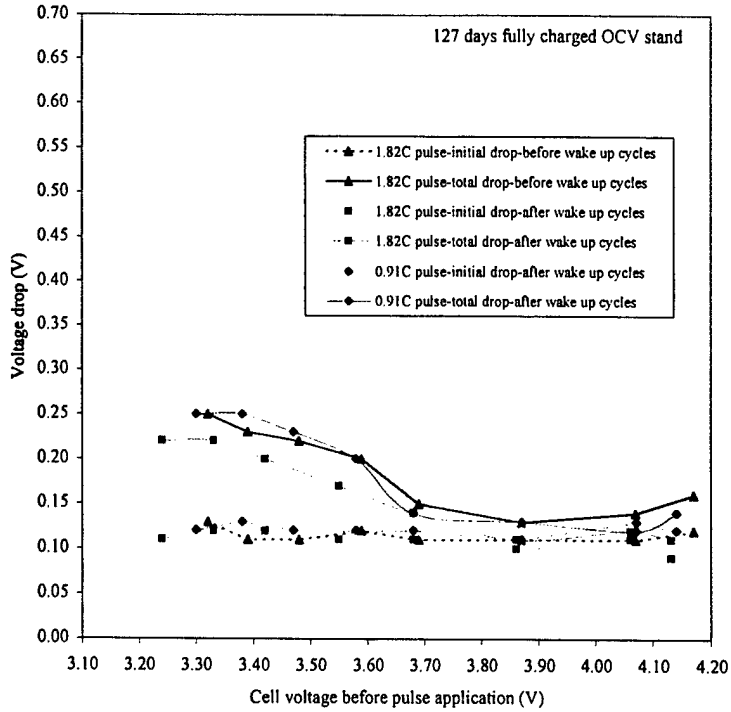

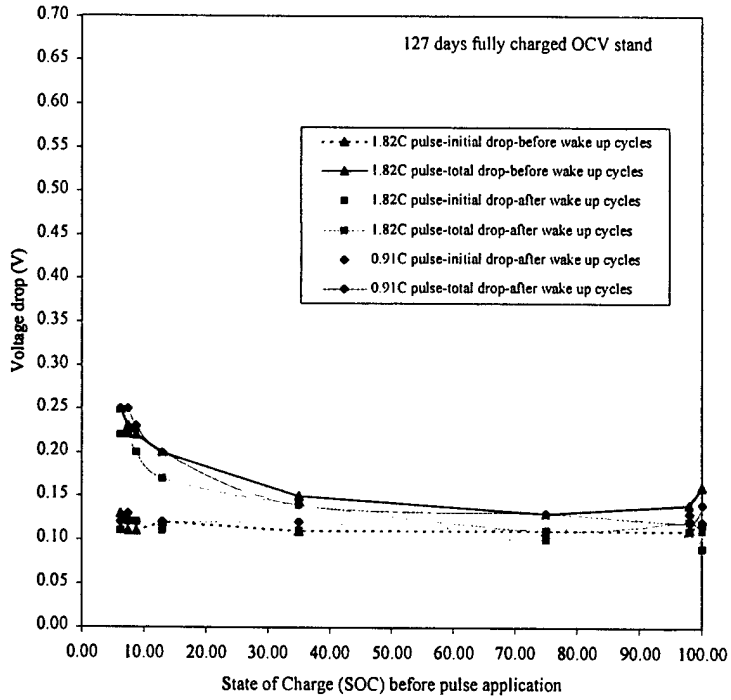

Figure 12. Plot presenting the instantaneous (0.01 s) and total (1 s) voltage drop after the application of pulse load in Sony SB-1 cell before and after the wake-up characterization cycles; (top) plot vs. voltage; (bottom) plot vs. SOC (±5%).

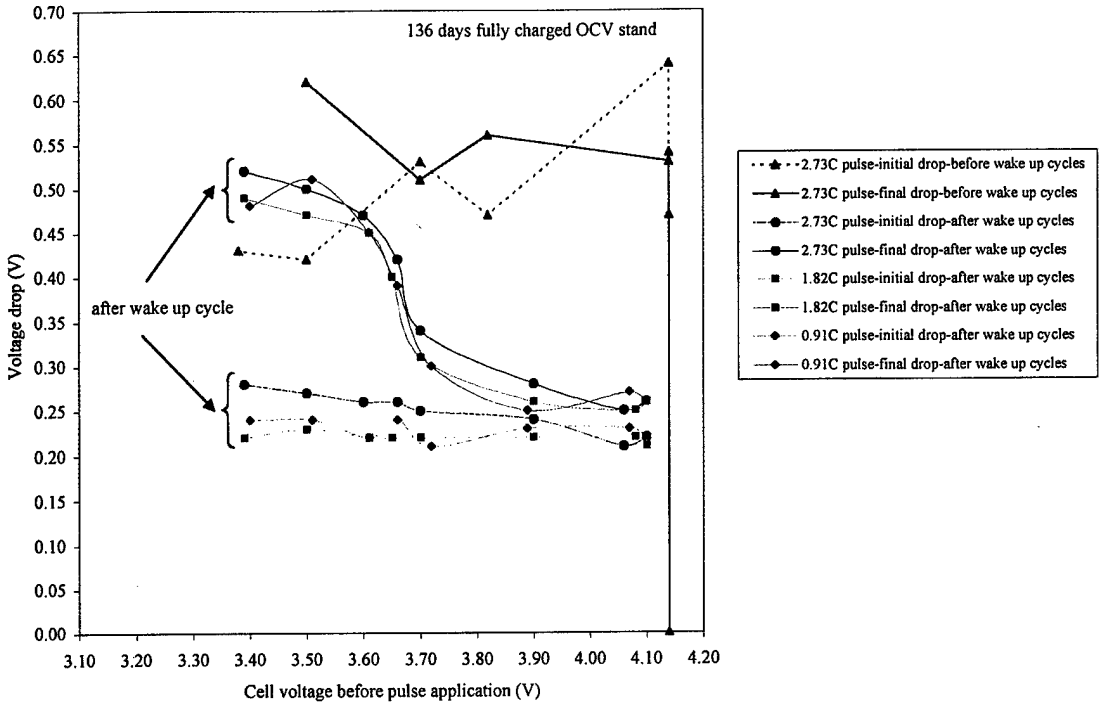

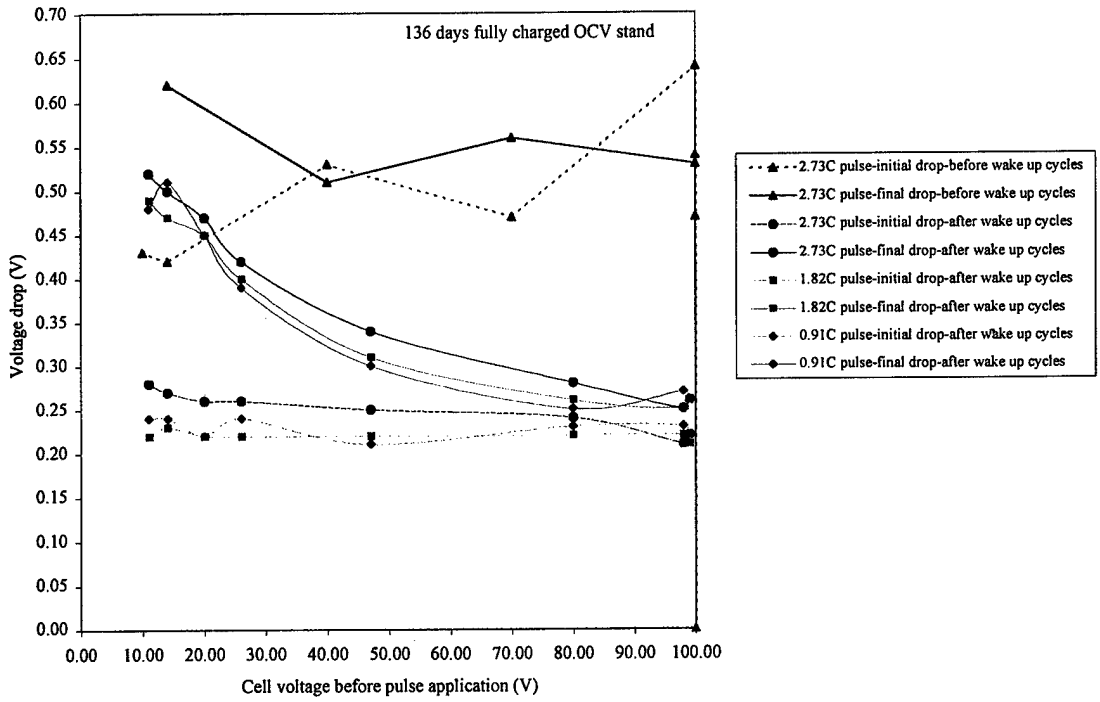

Figure 13. Plot presenting the instantaneous (0.01 s) and total (1 s) voltage drop after the application of pulse load in Canon (A&TB) CB-1 cell before and after the wake-up characterization cycles; (top) plot vs. voltage; (bottom) plot vs. SOC (±5%).

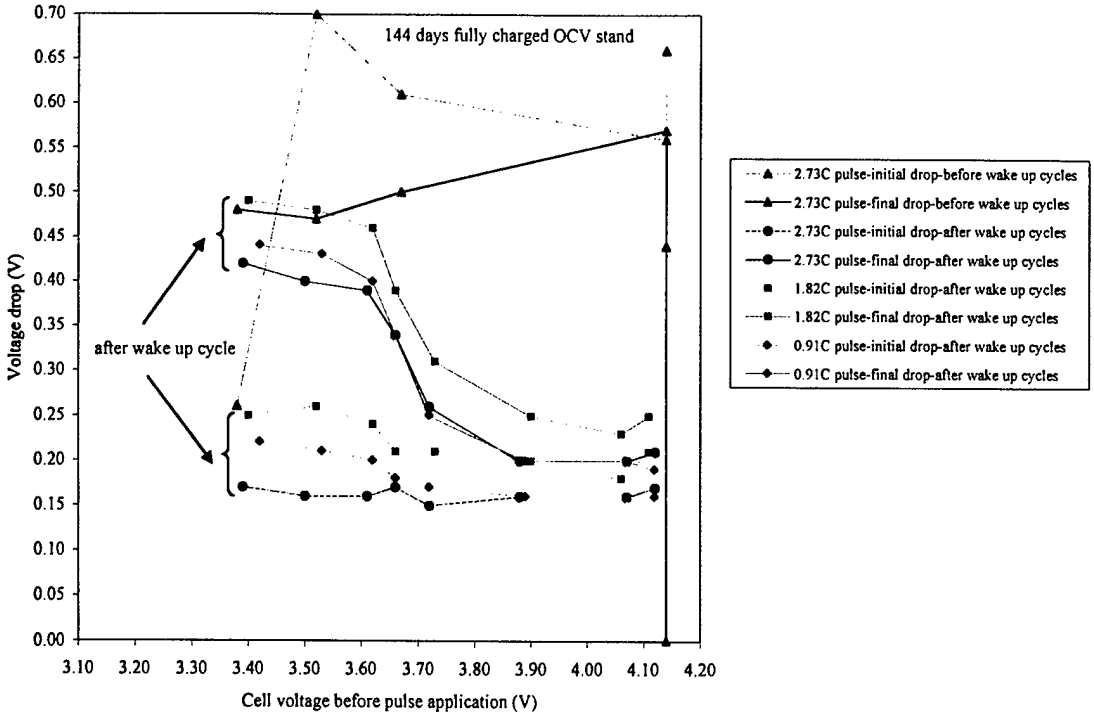

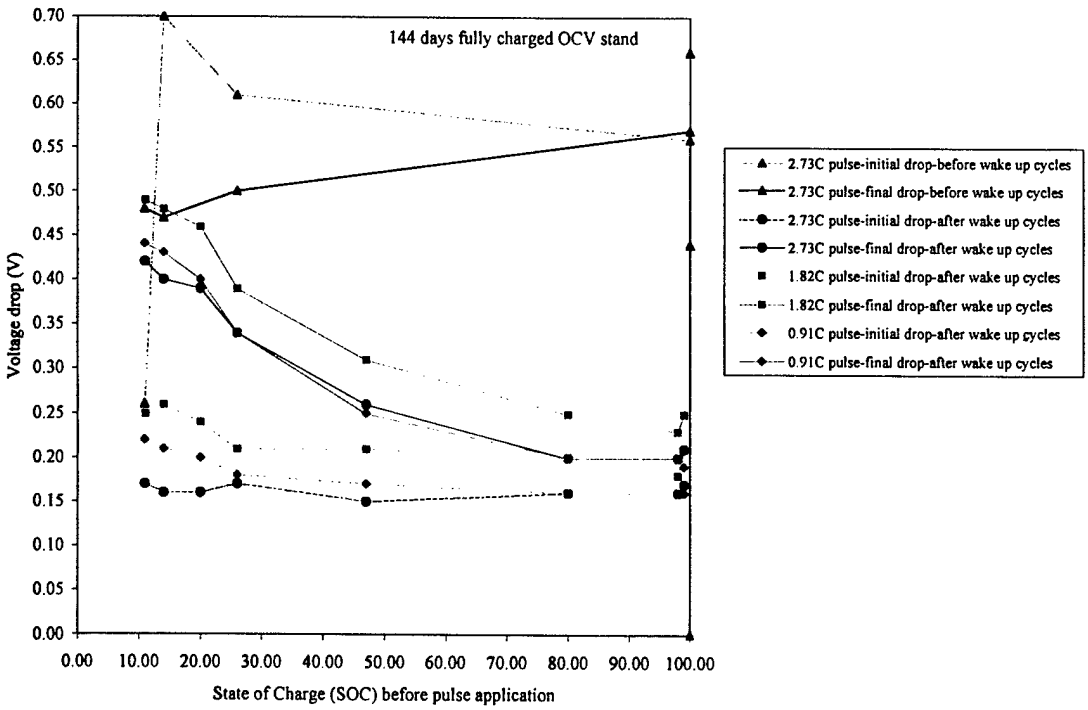

Figure 14. Plot presenting the instantaneous (0.01 s) and total (1 s) voltage drop after the application of pulse load in Canon (A&TB) CB-2 cell before and after the wake-up characterization cycles; (top) plot vs. voltage; (bottom) plot vs. SOC (±5%).

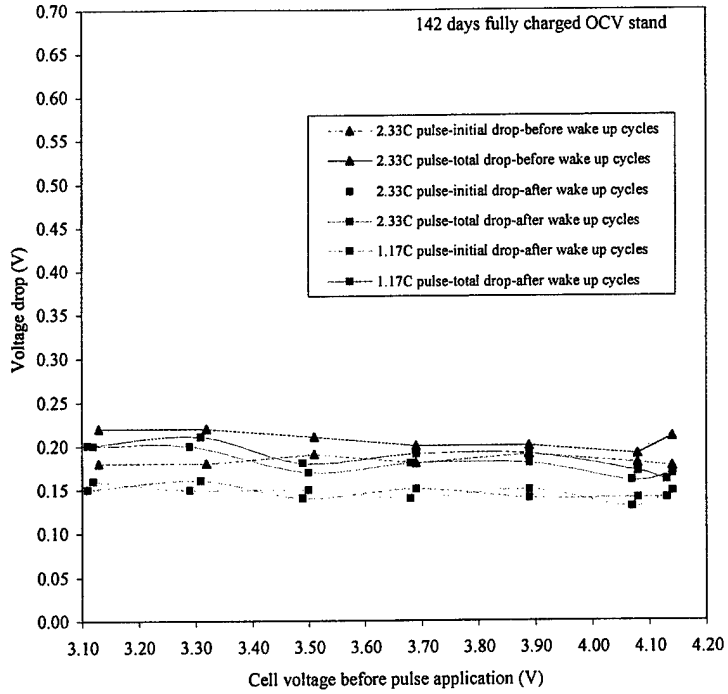

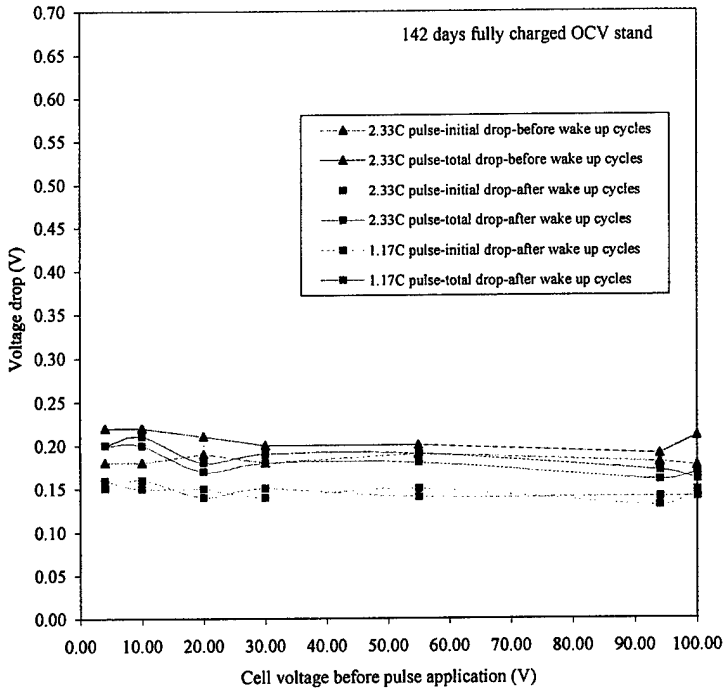

Figure 15. Plot presenting the instantaneous (0.01 s) and total (1 s) voltage drop after the application of pulse load in the space-grade cell before and after the wake-up characterization cycles; (top) plot vs. voltage; (bottom) plot vs. SOC (±5%).

The difference in aging behavior of Canon (A&TB) cells versus Sony and the space-grade cells may be related to the stability of electrodes with respect to reaction with electrolyte. The electrodes in Canon (A&TB) cells are believed to be more prone to oxidation and reduction reactions by electrolyte. Typically, the electrolyte reduction on the carbon electrode could take place due to finite electronic conductivity of the Solid Electrolyte Interface (SEI) layer.[1–3] During storage, this can lead to reaction of electrolyte with intercalated lithium within carbon and alter the SEI layer. Both self-discharge and decreased cycling performance after storage has been attributed to this effect. The anode-electrolyte side reactions are shown to be temperature dependent and could alter the SEI layer by changing parameters such as electronic conductivity and thickness over time.[4,5] Similar surface reactions can also take place at the cathode by oxidation of electrolyte.[6] Cathode oxidation reactions are typically voltage dependent and could lead to the formation of insoluble products such as Li_2CO_3.[6–8] These products are capable of precipitating on the electrodes surface and blocking the pores.[6] For Canon (A&TB) cells, the higher rate of self-discharge during storage (Figure 1) may be an indication of a greater electrode-electrolyte reactivity compared to that of Sony and the space-grade cells. Canon (A&TB) cells might be experiencing a greater amount of reaction products during aging on both the cathode and the anode due to this effect. Depending on the thickness and uniformity of these surface products, the ability to pass current during the pulse load could be affected. For the aged Canon cell before the wake up cycles, the first four steps involving a 200-mA charge to 4.2 V and 200-mA discharge to 4.0 V, 3.8 V, and 3.6 V, followed by a 3600-s OCV stand lead to similar cell voltages of 4.14 V before the application of pulse current. The cell voltage during each charge or discharge step reaches the EOCV or EODV limits very quickly, and the voltage stabilizes to 4.14 V during the OCV stand. This may be attributed to the presence of insulating films on the electrode surfaces formed during the storage period. Wake-up cycles are believed to break up these surface products, leading to a lower voltage drop and a more uniform and predictable response to pulse load. The Sony and space-grade cells are believed to have a more stable combination of electrodes and electrolyte, thus minimizing their reaction during the aging period, leading to more stable performance upon storage.

4. Final Remarks

The results of this work indicate a better pulse performance of Sony and the Space-grade cells compared to Canon (A&TB) battery cells. All cells showed a relatively small drop in voltage and good voltage stability due to pulse load, but Canon (A&TB) cells showed the largest drop in voltage with each pulse application. These cells also showed the greatest sensitivity to aging and a greater need to undergo re-conditioning for best performance and more reliable results. The voltage drop of Canon (A&TB) cells due to pulse load was highest and highly dependent on the aging condition. These cells also showed the greatest dependence on the state of charge with the largest voltage drop at $V < 3.6$ V. It is recommended that lithium-ion chemistries similar to that of the Canon (A&TB) battery cells be avoided for any high-rate applications where good voltage control under load is needed. The voltage drop of Sony cells showed a small dependence on the state of charge, but the effect of aging was minimal. The space-grade cells showed no dependence on the state of charge with negligible aging effect. The voltage drop during the pulse load was also found to be independent of the pulse rate for all the cells up to the maximum pulse current of 3 A examined in this work.

The results of this work indicate promising features of Sony and the space-grade cells for high-rate applications, with the space-designed cell chemistry exhibiting the best performance. It is recommended that these cells be further investigated at higher rates and different temperatures once a higher current power source with fast data acquisition capability becomes available. It is also recommended that the coke anode similar to that used in the space-designed cell be considered and further investigated for applications where stable voltage under high-rate load is needed. Additional investigation on the effect of storage conditions such as temperature and voltage on pulse performance would also give more insight to the aging mechanism and help determine the best storage conditions for these cells.

References

1. S. Eftekharzadeh, "Common Failure Modes in Lithium-ion Batteries," ATR 2003(8180)-1, Dec 2002.

2. E. Peled, *Lithium Batteries*, J.-P. Gabano Editor, P. 43, Academic Press, New York (1983).

3. A. M. Andersson and K. Edstrom, *J. of Electrochem. Soc.*, **148** (10) A1100-A1109 (2001).

4. M. Broussely, S. Herreyre, P. Biensan, P. Kasztejna, K. Nechev, R. J. Staniewicz, *J. Power Sources*, **97-98** 13 (2001).

5. J. Bloom, B. W. Cole, J. J. Sohn, S. A. Jones, E. G. Polzin, V. S. Battaglia, G. L. Henriksen, C. Motloch, R. Richardson, T. Unkelhaeuser, D. Ingersoll, H. L. Case, *J. Power Sources*, **101** 238 (2001).

6. R. Imhof and P. Novak, *J. Electrochem. Soc.*, **146** (5) 102 (1999).

7. R. Fong, U. von Sacken, and J. R. Dahn, *J. Electrochem Soc.*, **137** 2009 (1990).

8. Y. Ein-Eli, B. Markovsky, D. Aurbach, Y. Carmeli, H. Yamin, and S. Luski, *Electrochim. Acta*, **39**, 2559 (1994).

LABORATORY OPERATIONS

The Aerospace Corporation functions as an "architect-engineer" for national security programs, specializing in advanced military space systems. The Corporation's Laboratory Operations supports the effective and timely development and operation of national security systems through scientific research and the application of advanced technology. Vital to the success of the Corporation is the technical staff's wide-ranging expertise and its ability to stay abreast of new technological developments and program support issues associated with rapidly evolving space systems. Contributing capabilities are provided by these individual organizations:

Electronics and Photonics Laboratory: Microelectronics, VLSI reliability, failure analysis, solid-state device physics, compound semiconductors, radiation effects, infrared and CCD detector devices, data storage and display technologies; lasers and electro-optics, solid-state laser design, micro-optics, optical communications, and fiber-optic sensors; atomic frequency standards, applied laser spectroscopy, laser chemistry, atmospheric propagation and beam control, LIDAR/LADAR remote sensing; solar cell and array testing and evaluation, battery electrochemistry, battery testing and evaluation.

Space Materials Laboratory: Evaluation and characterizations of new materials and processing techniques: metals, alloys, ceramics, polymers, thin films, and composites; development of advanced deposition processes; nondestructive evaluation, component failure analysis and reliability; structural mechanics, fracture mechanics, and stress corrosion; analysis and evaluation of materials at cryogenic and elevated temperatures; launch vehicle fluid mechanics, heat transfer and flight dynamics; aerothermodynamics; chemical and electric propulsion; environmental chemistry; combustion processes; space environment effects on materials, hardening and vulnerability assessment; contamination, thermal and structural control; lubrication and surface phenomena. Microelectromechanical systems (MEMS) for space applications; laser micromachining; laser-surface physical and chemical interactions; micropropulsion; micro- and nanosatellite mission analysis; intelligent microinstruments for monitoring space and launch system environments.

Space Science Applications Laboratory: Magnetospheric, auroral and cosmic-ray physics, wave-particle interactions, magnetospheric plasma waves; atmospheric and ionospheric physics, density and composition of the upper atmosphere, remote sensing using atmospheric radiation; solar physics, infrared astronomy, infrared signature analysis; infrared surveillance, imaging and remote sensing; multispectral and hyperspectral sensor development; data analysis and algorithm development; applications of multispectral and hyperspectral imagery to defense, civil space, commercial, and environmental missions; effects of solar activity, magnetic storms and nuclear explosions on the Earth's atmosphere, ionosphere and magnetosphere; effects of electromagnetic and particulate radiations on space systems; space instrumentation, design, fabrication and test; environmental chemistry, trace detection; atmospheric chemical reactions, atmospheric optics, light scattering, state-specific chemical reactions, and radiative signatures of missile plumes.